C. R. Physique 12 (2011) 234–245

Contents lists available at ScienceDirect

Comptes Rendus Physique

www.sciencedirect.com

Gamma-ray burst studies in the SVOM era / Étude des sursauts gamma à l'ère de SVOM

Shock acceleration in gamma-ray bursts

Accélération de choc dans des sursauts gamma

Martin Lemoine [a,*], Guy Pelletier [b]

[a] *Institut d'astrophysique de Paris, CNRS – université Pierre and Marie Curie, 98, bis boulevard Arago, 75014 Paris, France*
[b] *Laboratoire d'astrophysique de Grenoble, CNRS – université Joseph-Fourier II, BP 53, 38041 Grenoble, France*

ARTICLE INFO

Article history:
Available online 9 March 2011

Keywords:
Gamma-ray bursts
Particle acceleration
Shock waves

Mots-clés :
Sursauts gamma
Accélération de particules
Ondes de choc

ABSTRACT

Gamma-ray bursts offer a rather unique window on the fundamental astrophysics of particle acceleration. Sources of high-energy gamma rays, they are also likely sources of cosmic rays, possibly of the so-called ultra-high energy cosmic rays, and they may well turn out to be the strongest sources of high energy neutrinos. Through the interaction of their outflow with the circum-burst medium, these explosions generate ultra-relativistic shock waves that convert part of the bulk kinetic energy into particle energy, ultimately giving rise to the impressive photon power law spectra of the afterglow. The prompt emission may well occur through the interactions of disturbances moving with mildly relativistic relative velocity within the flow itself. However, the detailed acceleration mechanism is not yet understood. This chapter discusses the progress made in the past decade in our understanding of relativistic shock acceleration and its relation to gamma-ray burst phenomenology. It notably discusses the intimate relationship between the electromagnetic micro-instabilities upstream of the collisionless shock and the accelerated particles. It also briefly discusses the possibility of accelerating particles to ultra-high energies and the production of secondary neutrino signals. It concludes with a list of open questions and some perspectives.

RÉSUMÉ

L'étude des sursauts gamma offre une perspective unique sur la physique des processus d'accélération dans les objets astrophysiques. Sources de photons gamma de haute énergie, les sursauts gamma sont probablement des sources de rayons cosmiques, peut-être même des fameux rayons cosmiques d'ultra-haute énergie ; et ils pourraient bien être les sources les plus puissantes de neutrinos de haute énergie. L'interaction du flot relativiste produit par l'explosion avec le milieu extérieur déclenche une onde de choc ultra-relativiste qui convertit l'énergie cinétique d'ensemble en énergie désordonnée de particules. Ce mécanisme conduit in fine aux remarquables distributions de photons en loi de puissances de la phase de rémanence du sursaut. L'émission prompte pourrait résulter d'interactions similaires entre perturbations animées de vitesses relatives modérément relativistes à l'intérieur du flot. Pour autant, le mécanisme fondamental d'accélération n'est pas compris dans ses détails. Ce chapitre discute des avancées récentes sur l'accélération de particules autour des ondes de chocs relativistes et du lien avec la phénoménologie des sursauts gamma. On discute en particulier le lien intime qui relie les micro-instabilités électromagnétiques en amont du choc non collisionnel aux particules accélérées. Ce chapitre discute brièvement l'accélération de particules aux ultra-hautes énergies ainsi que

1631-0705/$ – see front matter
doi:10.1016/j.crhy.2011.01.011

la génération possible d'un fond de neutrinos de très haute énergie. Enfin, on conclut par une liste de questions ouvertes et quelques perspectives.

1. Introduction

Gamma-ray bursts are exceptional astrophysical objects in many respects. In gamma rays they become the brightest objects in the sky on timescales of seconds, before fading away at longer wavelengths, on much longer timescales. Gamma-ray bursts may also be prominent sources of gravitational waves, at least for the short bursts that are expected to be related to the merging of compact objects. Gamma-ray bursts are also considered as the possible sources of the highest energy hadronic particles in Nature. And gamma-ray bursts are possibly the strongest astrophysical sources of PeV (and beyond!) neutrinos, that might be soon detected by upcoming experiments. These very high energy photons and neutrinos are produced as the secondaries of charged particles, that are accelerated through some mechanism that is yet to be elucidated. In that respect, gamma-ray bursts offer a unique perspective on the fundamental physics of particle acceleration in astrophysical objects, one of the central questions in high energy astrophysics. It is the aim of the present chapter to discuss some of the most salient issues related to particle acceleration, what we have learned and what we may expect to learn in the coming decade.

Observational progress in the field of gamma-ray burst studies has been quite remarkable, to the point where standard models, or paradigms, have emerged in the literature, see e.g. [1] for a detailed review and other sections in this volume. According to the standard lore, a central engine produces a ultra-relativistic flow with bulk Lorentz factor $\Gamma_{\rm w} \gg 1$. As this flow interacts at large radii with the circum-burst medium, either the wind of the parent star or the interstellar medium, it launches a ultra-relativistic shock wave which slowly decelerates as more matter is accreted from the external medium, and as more energy is dissipated in the reverse shock wave that propagates through the ejecta. The dissipation of energy in this external shock system is assumed to power the light-curve of the afterglow in a large band of wavelengths, as far as the radio domain. This secondary radiation obviously provides important clues as to the mechanism through which particles are accelerated at relativistic to ultra-relativistic shock waves, as will be discussed in the following.

If the flow originally contains inhomogeneities or fluctuations of the Lorentz factor at injection, one expects internal shocks to develop at intermediate radii. Such shock waves are expected to be mildly relativistic if the contrast between the Lorentz factors is not much greater than unity and they may be responsible for the erratic prompt emission observed in γ rays. There are alternative models for the prompt emission, however. For instance, if most of the flow energy is carried by electromagnetic fields, the dissipation that gives rise to the prompt emission might result from reconnection events within the flow [2]. A recent alternative is that of particle acceleration in relativistic turbulence [3], and yet another possibility is that of shear acceleration [4], whereby a particle gains energy through its interaction with a stratified velocity field, similar in a way to the mechanism of Fermi acceleration. This article will actually focus on Fermi mechanisms, and most notably on shock acceleration, as it is undoubtedly the most standard and most studied mechanism as well as one in which significant progress has been made in the past decade or so; it is also generally believed to be at the origin of the afterglow emission, if not of the prompt emission.

Bringing side to side the knowledge that we have acquired in our understanding of particle acceleration at relativistic shock waves and the observational results on gamma-ray burst radiation brings forward many open questions and interesting problems, the resolution of which will ultimately lead to further progress (and further questions!). The present article aims at discussing these questions, results and open problems. It is laid out as follows: in Section 2, we recall the fundamental physics at play in Fermi type acceleration; in Section 3 we briefly recall the physics of shock acceleration in the non-relativistic regime, which is much better understood than that in the relativistic regime, to be discussed in Section 4; we summarize the current state of the art of relativistic shock acceleration in Section 5; in Section 6 we discuss the generation of high energy γ rays, neutrinos and cosmic rays in gamma-ray bursts. Finally, in Section 7, we discuss the perspectives in this field.

2. Particle acceleration at collisionless shock waves

In a famous 1949 paper [5], Enrico Fermi set the ground for particle acceleration in astrophysics, discussing how cosmic rays can be accelerated to relativistic energies through their repeated interactions with moving magnetized structures. The basic principle is the following: the interaction of a particle with a magnetized structure is purely elastic in the rest frame of the structure, since any electric field is erased in the plasma rest frame thanks to the enormous conductivity of astrophysical plasmas; however, if the structures are moving in the laboratory frame, the motional electric field may lead to energy gains or losses; hence, ultimately, the efficiency of acceleration relies on the statistics of the velocity distribution of the moving structures and of the momentum transfer per interaction.

* Corresponding author.
E-mail addresses: lemoine@iap.fr (M. Lemoine), guy.pelletier@obs.ujf-grenoble.fr (G. Pelletier).

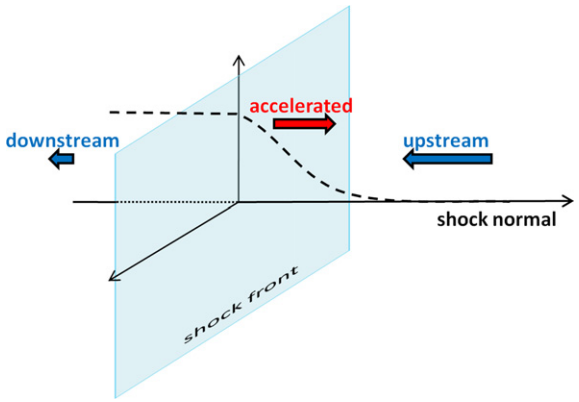

Fig. 1. Simplified shock geometry. As viewed in the shock front rest frame, the unshocked upstream medium is approaching at velocity $\beta_{\rm sh}c$ from the right, and the bulk kinetic energy is dissipated in heat and compression in the shocked downstream medium, which moves away from the shock at a smaller velocity $\beta_{\rm d}c$. The dashed line represents a schematics of the accelerated particle density along the shock normal, with some decreasing density profile in front of the shock wave; this region constitutes the shock precursor.

In the original Fermi mechanism, scattering is purely stochastic, leading to the so-called second order Fermi process, second-order meaning that the mean energy change at each interaction $\langle \Delta E\rangle/E \propto \beta^2$, with βc the average velocity of the scattering centers. Obviously, if the scattering agents move relativistically with $\beta \sim 1$, this second order mechanism may become as efficient as the first order Fermi mechanism discussed below [6]. This stochastic scattering can be generalized to the process of turbulent acceleration, in which particles gain energy by interactions with turbulent plasma waves, the statistics of energy gain then being related to the power spectrum of the turbulence, e.g. [7].

By working out the energy gain through the interaction with a moving disturbance, one can note that effective energy gain (loss) occurs when the parallel momentum transfer is opposite to (directed along) the velocity of the disturbance, or, in practice if the disturbance is converging toward (diverging away from) the particle. In other words, in a flow that presents a net converging velocity field, i.e. $\boldsymbol{\nabla}\cdot\boldsymbol{\beta} < 0$, then the energy gain can be important, all the more so when the particles can be repeatedly scattered in the region of converging flow. This is the first order Fermi process, for which $\langle \Delta E\rangle/E \propto \beta$.

Such a structure is encountered at a shock front, as depicted in Fig. 1. Consider a ultra-relativistic flow with bulk Lorentz factor $\Gamma_{\rm rel}$ (velocity $\beta_{\rm rel}c$ as measured in the laboratory frame) launching a shock wave with shock Lorentz factor $\Gamma_{\rm sh}$ (velocity $\beta_{\rm sh}c$) in a medium that is initially at rest, dubbed the upstream medium. As viewed from the rest frame of the shock front, the unshocked (upstream) medium converges towards the shock interface from upstream plus infinity with bulk Lorentz factor $\Gamma_{\rm sh}$, while the downstream (shocked) medium moves toward downstream negative infinity with velocity $\beta_{\rm d}c$ (with $\beta_{\rm d} \sim 1/3$ in the unmagnetized strong relativistic shock limit). The choice of terms, upstream vs downstream, is directly related to the streaming motion in this shock rest frame. The unshocked medium forms a cold ultra-relativistic beam, the kinetic energy of which is dissipated through heating and compression on shock crossing. The characteristics of the particle populations on both sides of the shock are related to one another through the shock crossing conditions, that express the conservation of conserved quantities (current and energy–momentum). By inspection of Fig. 1, or of the velocity profile, it is easy to see that this shock structure possesses the characteristics of a converging flow, $\boldsymbol{\nabla}\cdot\boldsymbol{\beta} < 0$, which makes first order Fermi acceleration possible.

3. The non-relativistic regime: particle acceleration in supernovae remnants shock waves

It is instructive to discuss first the case of acceleration at non-relativistic collisionless shock waves, as observed in supernovae remnants.[1] This subject has been studied in detail for about three decades now, and a wealth of high accuracy observational data exist, that have brought valuable information on acceleration physics.

Like most supersonic outflows, the flow resulting from a supernova explosion produces a terminal shock in the interstellar medium (ISM) that propagates at a velocity of several 10^3–10^4 km/s and produces also a reverse shock that propagates in the ejecta. These two shocks are separated by a "working surface" which is a contact discontinuity; the fast external shock appears the most efficient for particle acceleration. The ISM mean field is quite weak ($\simeq 3$ μG), hence the magnetization parameter – an important parameter of the physics of relativistic shocks – is quite low: $\sigma_{\rm u} \equiv B^2/(4\pi\rho_{\rm ISM}m_p c^2) \sim 10^{-9}$. There exist strong evidence that the Fermi process works at those shocks, as notably imaged by X-ray, γ-ray and even TeV γ-ray telescopes in nearby supernovae remnants. In particular, spectra collected by the HESS telescope reveal photon power laws extending to 10–100 TeV with differential energy spectra $\mathrm{d}N_\gamma/\mathrm{d}\epsilon_\gamma \propto \epsilon_\gamma^{-s_\gamma}$ of index s_γ only slightly larger

[1] The shock is said collisionless because the transition from the unshocked to the shocked state takes place on a length scale that is much smaller than a collisional mean free path; the transition is then mediated by collective plasma effects. This is a generic situation in astrophysics, given the low densities found in astrophysical environments.

than 2, e.g. [8], which agree relatively well with the predictions of non-relativistic shock acceleration, discussed hereafter. Furthermore, the most recent data of SN1006 by the HESS Collaboration [9] has been interpreted as providing evidence for π^0-decay, indicating acceleration of ions to energies beyond 10 TeV [10].

In the test particle limit, in which one neglects the back-reaction of the accelerated particles on the shock structure, one can provide a simple analytical description of the acceleration process [11,12]. Suprathermal particles, that have a mean free path much larger than the thickness of the shock, undergo scattering off frozen magnetic perturbations on both sides of the shock and gain energy by making wandering cycles back and forth. By following the particle along one cycle, i.e. from upstream to downstream and then back to upstream, using appropriate Lorentz transforms to go to the rest frame of the plasma with which the particle interacts (elastically in this frame), one can show that the energy gain per cycle

$$\frac{\Delta E}{E} = \Gamma_{\rm rel}^2(1+\beta_{\rm rel}\cos\theta_{\rm d\to u})(1-\beta_{\rm rel}\cos\theta_{\rm u\to d})-1 \tag{1}$$

This formula [5] is quite general and will be useful in the relativistic limit discussed in the next section: here, in the non-relativistic limit, the relative velocity between upstream and downstream $\beta_{\rm rel}\simeq\beta_{\rm u}-\beta_{\rm d}\ll 1$ (with the upstream $\beta_{\rm u}c$ and downstream $\beta_{\rm d}c$ velocities measured relatively to the shock front, so that $\beta_{\rm u}=\beta_{\rm sh}$) and the associated Lorentz factor $\Gamma_{\rm rel}\simeq 1$. The angle $\theta_{\rm d\to u}$ (resp. $\theta_{\rm u\to d}$) corresponds to the angle between the particle momentum and the shock normal at shock crossing from downstream (resp. upstream) towards upstream (resp. downstream), as measured in the upstream (resp. downstream) plasma rest frame. Through flux weighted averaging over these angles, one obtains the average energy gain per cycle up $\to$ down $\to$ up, $\langle\Delta E\rangle/E=4(\beta_{\rm u}-\beta_{\rm d})/3$, and for a strong non-relativistic shock $\beta_{\rm u}=4\beta_{\rm d}$. These cycles are repeated until the particle escapes far downstream with a probability $P_{\rm esc}=\beta_{\rm u}\ll 1$. Note that the particle cannot escape upstream in the present approximation of an infinite planar shock wave of infinite lifetime, as it is bound to return to the shock in a finite amount of time. While downstream, the particle may escape as the flow moves away from the shock front, but its large return probability $1-P_{\rm esc}$ ensures that it will undergo many Fermi cycles. Finally, this interplay between energy gains and losses leads to the generation of a universal power law distribution of particle energy. Indeed any particle energy ϵ can be reached after at least n Fermi cycles, with n such that: $\epsilon=G^n\epsilon_0$ ($G\equiv 1+\langle\Delta E\rangle/E$ and ϵ_0 the initial energy); the probability for undergoing at least n cycles is $P_n=(1-P_{\rm esc})^n$, hence by eliminating n between these two quantities, one finds an energy spectrum $\mathrm{d}n/\mathrm{d}\epsilon\propto\epsilon^{-s}$ with

$$s=1-\frac{\ln(1-P_{\rm esc})}{\ln(1+\Delta E/E)}\simeq 1+\frac{3}{r-1} \tag{2}$$

with r the compression ratio of the shock. So a strong non-relativistic shock ($r=4$) produces a power law cosmic ray spectrum with index $s\simeq 2$ in this test particle limit. The spectrum index is the same for relativistic electrons and protons, but the cut off caused by energy losses are different. The relativistic electrons lose energy through synchrotron radiation and the power law spectrum displays an exponential drop when the electron energy is such that the energy gain during a Fermi cycle becomes smaller than the energy loss. As for the protons, their maximal energy $E_{\rm max}$ is limited by the age of the shock wave, that the acceleration timescale to $E_{\rm max}$ cannot exceed. Determining the exact value of $E_{\rm max}$ is a hot topic in this field. Famous arguments dating back to [13] indicate that it is very difficult to increase this energy up to $\sim 10^{15}$ eV, which is desired from a purely phenomenological point of view, as the cosmic ray spectrum appears featureless up to that energy.

The above description of Fermi acceleration has been substantially improved in the past decades. First of all, it has been realized that the test particle approximation is inadequate as the accelerated particle population dominates the upstream fluid pressure so that its back-reaction cannot be neglected. This has led to the elaboration of non-linear Fermi acceleration models, in which the flow structure is solved more or less self-consistently with the inclusion of particle acceleration [14]. More recently, detailed X-ray images of the rims of supernovae remnants shock waves have provided constraints on the downstream magnetic field. Surprisingly enough, it appears to exceed the interstellar magnetic field by one to two orders of magnitude, after accounting for compression through the shock transition [15]. The origin of this amplified field remains subject to interpretation but there is a growing consensus that the agents of the amplification are the accelerated particles themselves. It has been long known indeed that the anisotropic distribution of the fast particles may trigger instabilities in the shock precursor (see Fig. 1), leading to magnetic field amplification in the upstream medium [16]. Two generic types of instabilities have been discussed in the recent literature: one results from a resonance between the Larmor motion of cosmic rays with the spatial modulation of waves with right or left polarization; the other is of a purely non-resonant nature and is associated to the disturbance of the return current seeded in the background unshocked plasma by the current carrying cosmic ray beam [17]. It seems that a combination of both (and possibly more) seems required at supernovae remnant shock waves [18–20]. In our discussion of relativistic shocks further below, similar instabilities will emerge as fundamental action players.

If a supernova explosion can convert 10% of its shock kinetic energy into cosmic ray energy – a reasonable approximation – and if the magnetic field can be amplified to the above inferred values, then these objects may well account for the bulk of cosmic rays, with a maximal energy of the order of the so-called knee, a very desirable feature indeed.

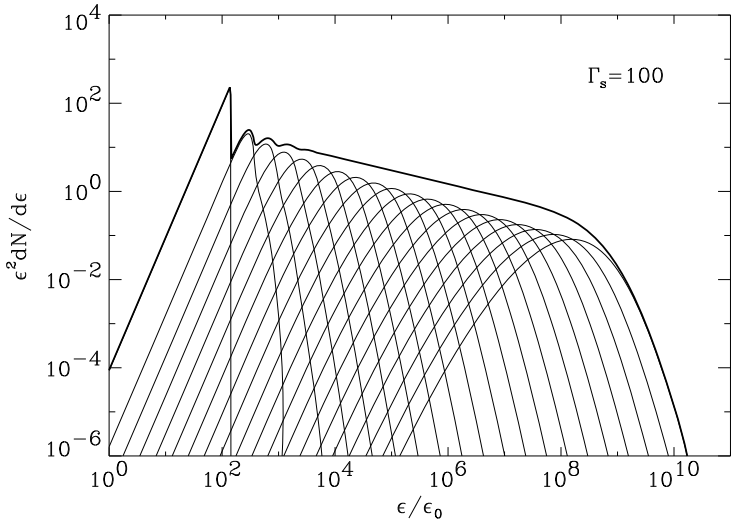

Fig. 2. Spectrum of particles escaping downstream (thick line) as a function of momentum after 20 cycles for $\Gamma_{\rm sh} = 100$; in thin lines, the spectra of particles escaping downstream after each cycle [26].

4. Particle acceleration at relativistic shock waves

Around the beginning of the century, several new results appeared in the literature pointing to prominent differences between the Fermi mechanisms in the relativistic and non-relativistic limits, yet indicating that relativistic shock acceleration is efficient, leading to power law spectra with a universal slope $s \simeq 2.3$. These studies concluded to a sub-Larmor acceleration timescale, which opens the way to acceleration up to the maximum limit allowed by the size of the cosmic accelerator, quite a noteworthy feature of relevance to the generation of the highest energy cosmic rays.

The most striking difference with respect to non-relativistic test particle Fermi acceleration is that the shock wave moves about as fast as the accelerated particle, hence it never lies far behind it [21,22]. Recall for instance that for $\Gamma_{\rm sh} \gg 1$, $\beta_{\rm sh} \simeq 1 - 1/2\Gamma_{\rm sh}^2$ so that after a time t, the distance between the particle and the shock wave cannot exceed $ct/(2\Gamma_{\rm sh}^2)$. This observation has several important consequences. First of all, the accelerated particle does not have time to diffuse in the unshocked medium before returning to the shock front, it cannot even turn back on itself but is rather caught back by the shock front as soon as the particle velocity along the normal to the shock front falls below $\beta_{\rm sh}c$, i.e. as soon as it is deflected by an angle of order $1/\Gamma_{\rm sh}$. Using Eq. (1), one can show that this implies an energy gain of a factor ~ 2 instead of $\Gamma_{\rm rel}^2$, as would otherwise be expected [21,22]. Although, at injection, the particle comes from upstream with an arbitrary angle, hence for the first up $\rightarrow$ down $\rightarrow$ up cycle, the gain is indeed $\Gamma_{\rm rel}^2$. As an aside, one may note that injection never is a problem for relativistic shocks, as compared to non-relativistic shocks: the cold upstream ion population is heated on shock crossing to $\Gamma_{\rm sh} m_p c^2$ energies as measured in the downstream rest frame; since the shock wave moves away from that rest frame at sub-relativistic velocities $\sim c/3$, a sizable fraction of the heated population is able to return upstream, with an energy $\sim \Gamma_{\rm sh}^2 m_p c^2$ in this upstream rest frame. If electrons thermalize downstream with the incoming ions, they are expected to be heated to Lorentz factors of order $\Gamma_{\rm sh} m_p/m_e$; this has been confirmed by recent Particle-In-Cell (PIC) simulations of relativistic electron–proton oblique shocks [23].

Early simulations of particle acceleration at relativistic shocks relied on Monte Carlo simulations of test particle propagation in pre-defined upstream and downstream turbulence [24–29]. Most simulations then converged towards a slope $s \simeq 2.3$ as $\Gamma_{\rm sh} \gg 1$, in agreement with semi-analytical [30] and analytical developments [31]. An example of such simulations is shown in Fig. 2, which shows the various sub-populations that escape downstream after a certain number of Fermi cycles. The addition of these populations, shown in thick solid line, produces the power law of the accelerated particle population.

However, that value $s \simeq 2.3$ corresponds to simplified hypotheses of isotropic turbulence, no mean field, with random jumps of the pitch angle during scattering, without following the phase of the magnetic field line in the shock front plane at shock crossing. As it turns out, these simplifications are too drastic and their revision has led to a refined picture of the relativistic Fermi process. In particular, it has been realized through numerical simulations [32,33] and analytical calculations [34] that the existence of a mean field or of turbulence organized on large spatial scales actually inhibit Fermi acceleration. Indeed, a relativistic shock with a mean field is generically "superluminal", meaning that the anchor point of a magnetic field line on the shock front moves faster than light along the shock front (in the shock front frame). This phenomenon takes place as soon as the angle of the field line Θ_B with respect to the shock normal exceeds $1/\Gamma_{\rm sh}$ in the upstream rest frame, since the magnetic component along the shock front in the shock front rest frame is $\Gamma_{\rm sh}$ times that in the upstream medium. A long established result implies that in this superluminal configuration, for a fully regular magnetic field, Fermi power law spectra do not develop [35]. In the case of turbulence spectra with coherence scales much larger than the typical

Larmor radius of the accelerated particle, this result remains unchanged [33,34]: particles can cross the shock front at most three times before being advected toward downstream minus infinity.

This effect had not been seen in early Monte Carlo simulations that described random pitch angle jumps and did not follow the phase of the magnetic field in the shock front plane through shock crossing. Yet, this result has several important consequences.

First of all, the so-called canonical slope $s = 2.3$ is not supported by theory and its precise value remains open. How does Fermi acceleration work in the relativistic regime, what power law does it produce are fundamental questions now being actively studied. Let us note, however, that the synchrotron interpretation of gamma-ray burst afterglows suggests that shock acceleration operates in the relativistic regime and produces power laws over several decades, see e.g. [1] for a detailed review.

Furthermore, in order for Fermi acceleration to proceed and develop power law spectra, it is necessary to excite electromagnetic turbulence on microscopic length scales (microscopic as compared to the typical Larmor radius of the accelerated particles). For reference, indeed, if one assumes that the gamma-ray burst external shock propagates in the interstellar medium, with ambient magnetic field $B \sim 3$ μG, the Larmor radius of downstream protons is $r_{\mathrm{L},0} \sim 10^{12}$ cm, very small indeed when compared to the typical length scales of the problem: $R \sim 10^{17}$ cm the shock radius of the afterglow, $\ell_B \gtrsim 10^{20}$ cm the coherence scale of the interstellar magnetic field.

Interestingly, the amplification of a pre-existing background magnetic field finds strong support in the interpretation of existing gamma-ray burst observations. It has been known for some time that, in order to fit the observed power laws with a synchrotron model, one needs a magnetic field that is only marginally sub-equipartition, with a ratio of magnetic to downstream thermal energy density $\epsilon_B \sim 10^{-3}$–10^{-1} [36,37], see also [1] for a detailed review. By contrast, the interstellar medium can contribute only $\epsilon_B \sim \sigma_{\mathrm{u}} \sim 10^{-9}$, hence it is necessary to assume efficient amplification of the ambient magnetic field. Since most radiating electrons are found downstream, the above result applies to downstream only, strictly speaking. However, by considering the acceleration timescale needed to produce electrons capable of radiating X-rays and gamma rays through synchrotron radiation, one can show that the upstream magnetic field must have been amplified by at least two to three orders of magnitude [38,39], unless of course, the circum-burst medium has been originally magnetized to that level by stellar winds.

Theory and observations thus meet at this point: relativistic Fermi acceleration develops at gamma-ray burst external shock waves with very strong amplification of the magnetic field on very short length scales. As we discuss in the following section, this opens a new avenue of research, which ties together the very structure of relativistic collisionless shock waves with the very mechanism of particle acceleration and the radiative processes.

5. Relativistic shock waves and acceleration: state of the art

As discussed above, successful Fermi acceleration at relativistic shock waves requires strong turbulence to develop on short spatial scales. How strong and on what scales exactly should this turbulence develop has been quantified by [40] by the means of analytical description of particle propagation in a short scale turbulence with a mean field. The accelerated particle must obey $\ell_{\mathrm{c}} \ll r_{\mathrm{L}} \ll \ell_{\mathrm{c}} \delta B/B$, where δB represents the microscopic turbulent magnetic field, ℓ_{c} its scale of coherence, B the large scale field and r_{L} the Larmor radius of the particle in the total magnetic field. The above inequality is written in the downstream rest frame.

In the absence of any external agent capable of magnetic amplification, the prime suspects for the generation of the microscopic electromagnetic turbulence are the accelerated particles themselves. In effect, as particles return from downstream toward upstream, they constitute a tenuous beam of charged particles of very small angular dispersion ($\lesssim 1/\Gamma_{\mathrm{sh}}$ as imposed by kinematics) and with velocity strongly peaked close to c. Such a beam can trigger beam–plasma instabilities in the upstream medium. In that respect, the situation is reminiscent of supernovae remnant shock waves, discussed in Section 3. Yet the relativistic nature of the shock wave forbids the development of large scale gyro-resonant instabilities. Indeed, as already mentioned the shock wave is always trailing right behind the accelerated particle, so that the effective penetration length scale (in the upstream frame) does not exceed $r_{\mathrm{L},0}/\Gamma_{\mathrm{sh}}^3$ [41] (with $r_{\mathrm{L},0}$ the Larmor radius calculated relatively to the pre-existing ambient magnetic field). This length scale also determines the maximum growth time available for instabilities to grow, before the plasma mode crosses the shock front, hence the pre-existing mean field puts a drastic limitation for the growth of the instabilities: only the fastest can grow.

These two points make the physics of Fermi process in relativistic regime extremely challenging. The shock structure, the generation of micro-turbulence and particle acceleration emerge as three inseparable facets of relativistic shock physics, which by itself represents an outstanding example of collisionless dissipative phenomena. This hot topic in the field of kinetic theory, has sparked the development of massive Particle-In-Cell (PIC) numerical simulations. These numerical codes solve directly the Maxwell equations for a large set of macro-particles and as such, they are best suited for addressing the interplay between particles and waves, which lies at the heart of relativistic shock formation and particle acceleration.

By now, such simulations are able to simulate the formation of a relativistic shock wave through the instabilities triggered by the interpenetration of two plasma flows in two or three dimensions with nearly realistic proton to electron mass ratio and for various magnetization levels, e.g. [44–46,43,47–50,23]. Some of these simulations have actually demonstrated the relevance of Fermi acceleration at unmagnetized relativistic shocks in pair plasmas [43], in electron–ion plasmas [49] and at magnetized subluminal relativistic shocks waves [50,23], see also Fig. 3 for an illustration. In the unmagnetized case,

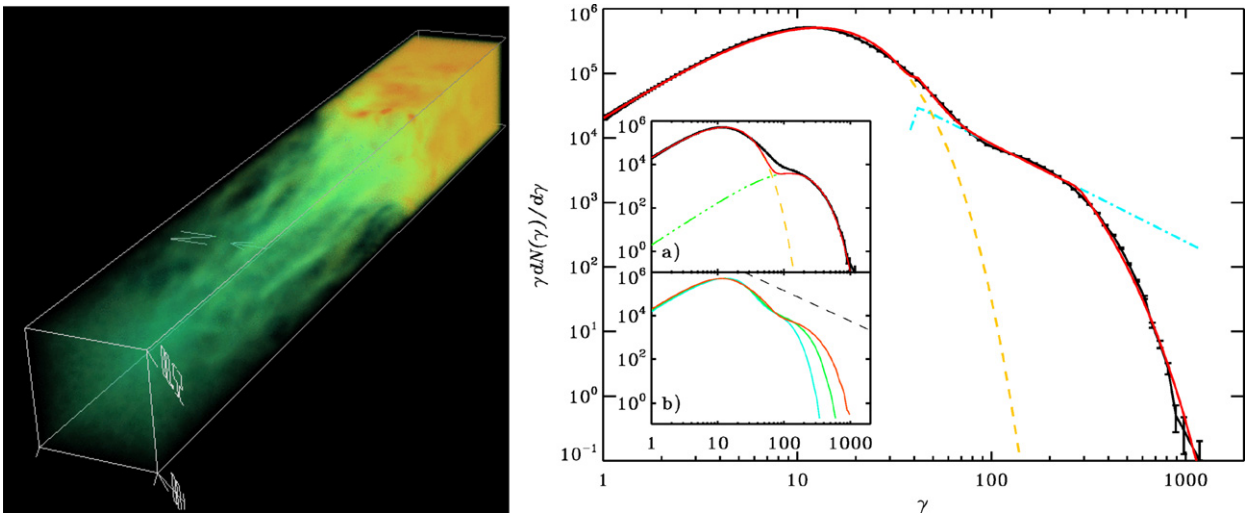

Fig. 3. Left panel: density profile at a relativistic shock wave moving with Lorentz factor $\Gamma_{\rm sh} \simeq 21$ in an unmagnetized pair plasma; at the upper right, the downstream thermalized medium, at the lower left, the unshocked upstream; the intermediate filamentary structure reveals the growth of instabilities in the shock precursor; figure taken from [42]. Right panel: energy spectrum as measured downstream, revealing the relativistic thermalized population with a high energy power law tail, limited in maximal energy by the run time of the simulation; figure taken from [43]. Courtesy A. Spitkovsky.

the ab initio simulations show that a shock front rises because of the reflection of a fraction of the incoming particles on the gradient of magnetic waves generated by the reflected particles themselves. One key instability in the formation of that collisionless structure is identified as the filamentation (also referred to as Weibel) instability, a well-known kinetic instability triggered by a beam pervading a plasma that generates purely magnetic fluctuations at short scales (electron inertial scale $\delta_{\rm e} \equiv c/\omega_{\rm pe} \sim 5 \times 10^5 n_0$ cm, with n_0 the upstream density in units of cm^{-3}) [51–54]. This filamentation instability produces characteristic patterns of high density magnetized filaments, as observed immediately upstream of the shock front, clearly seen in the top panel of Fig. 3.

As stated earlier, only the fastest instability modes can grow, but the paraphernalia of relevant instabilities is not limited to the Weibel instability [55]. The well-known ordinary two stream instability may be of relevance in the mildly relativistic limit, as its growth rate is large but suppressed by $\Gamma_{\rm sh}^{-4/3}$. A recently discovered oblique variant, of direct relevance in inertial confinement fusion research [56], offers a much larger growth rate. Čerenkov resonant instabilities with the upstream plasma eigenmodes, in particular with Whistler waves, also offer large growth rates [57]. These micro-instability modes generally find their strongest growth on the upstream skin depth scale δ_e. Yet, at larger (MHD) scales, [40] have observed the development of an instability produced by a net current of accelerated particles interacting with an oblique magnetic field, while in parallel shock waves, the relativistic generalization of the Bell instability may become relevant [41,58]. Which instability prevails is currently the subject of active research.

One may note that the simulations of [50,23] confirm the results discussed in Section 4, namely that a superluminal configuration prohibits Fermi power law spectra in the absence of short scale turbulence, but that these power law emerge in a non-perpendicular subluminal configuration. Since the superluminal case remains generic in the relativistic limit $\Gamma_{\rm sh} \gg 1$ – let us recall indeed, that the shock is superluminal when the angle between the magnetic field direction and the shock normal $\Theta_B > 1/\Gamma_{\rm sh}$ – one needs to understand how the existing mean field inhibits Fermi acceleration and at which low magnetization levels instabilities may grow. At present, our understanding of the structure of relativistic shock waves and of the possibility of Fermi acceleration can be recapped as follows.

- At mildly relativistic shock waves, meaning $\Gamma_{\rm sh} \sim a$ few, the subluminal configuration is equally probable and therefore Fermi acceleration should not be inhibited by the pre-existing mean field. Although the expectations are overall optimistic, very little is known of Fermi acceleration and of the development of instabilities in that regime. Much work needs to be done in this respect, as mildly relativistic shocks may well be at the origin of the prompt emission in gamma-ray bursts.
- At ultra-relativistic unmagnetized shock waves, Fermi acceleration is to take place through scattering in the micro-turbulence that the accelerated particles themselves generate. The fastest instability mode in this case appears to be the oblique two stream mode mentioned earlier [57]. Although this instability triggers mainly electrostatic modes, it may lead to efficient scattering through a second order Fermi process. Its role with respect to the shock mediation remains however to be elucidated through detailed PIC simulations.
- At ultra-relativistic (oblique) magnetized shock waves with a strong enough magnetic field, i.e. with upstream magnetization $\sigma_{\rm u} > \sigma_{\rm crit}$, even micro-instabilities cannot grow because the shock precursor is too short, i.e. the instabilities do not have time to grow on the shock precursor crossing timescale. The reflection of incoming particles may nevertheless

create a ring in phase space that triggers a maser synchrotron instability [59]. This instability in turn produces a precursor wave that travel upstream and that may lead to electron wakefield acceleration[2] in an electron–proton upstream plasma [61,62]. The relevance of this wakefield acceleration for gamma-ray burst phenomenology remains however to be elucidated.

– Below $\sigma_{\rm crit}$, micro-instabilities develop and allow Fermi acceleration to proceed. Actually, $\sigma_{\rm crit}$ takes a different value for each instability mode, a value that can be calculated by comparing the growth timescale with the transit time across the shock precursor. Here as well, the fastest mode seems to be the oblique mode, or rather its generalization to magnetized plasmas: the Čerenkov resonance of the beam with electrostatic modes that propagate along the magnetic field [57]. There exists an intermediate regime governed by the generation of whistler waves when the magnetization is weak and the Lorentz factor not too large, see [57].

In order to make contact with gamma-ray burst phenomenology, it is essential to understand the radiation signatures of Fermi acceleration. One immediate consequence of the above developments is that the traditional picture of synchrotron radiation has to be revised, as the magnetic field is distributed on sub-Larmor scales, with a possible non-trivial topology. In this respect, one may recall that relativistic electrons of Lorentz factor γ radiate toward the observer when their momentum points toward the observer within an angle $1/\gamma$ and that a random magnetic field of coherence length ℓ_c produces a relative transverse variation of the electron momentum a/γ when the electron travel over a coherence length, introducing the "wiggler" parameter $a \equiv e\bar{B}\ell_c/(m_e c^2)$. The meaning of this latter quantity is such that: when $a < 1$ the electron trajectory can display wiggles within the emission cone of angle $1/\gamma$, which leads to the "jitter radiation" regime investigated in [63] and subsequent papers. On the contrary, for $a > 1$ the electron crosses the emission cone from time to time without wiggling and thus radiates like in ordinary synchrotron emission. Both upstream and downstream, the wiggler parameter appears to be large [respectively $\epsilon_B^{1/2}(m_p/m_e)^{1/2}$ and $\epsilon_B^{1/2}\Gamma_{\rm sh}(m_p/m_e)$, with ϵ_B the fraction of downstream thermal energy density stored in electromagnetic micro-turbulence]. Therefore, despite the short scale variations of the magnetic field, one should expect the radiation to look like ordinary synchrotron emission, albeit without substantial polarization.

All of the above discussion has focussed on the micro-physics of relativistic Fermi acceleration, but it is instructive to consider the situation from a broader perspective, in particular that of the observer. Then, the synchrotron interpretation of the afterglow suggests $\epsilon_B \sim 10^{-3}$–10^{-1} over most of the emitting region, i.e. the blast wave of size $R/\Gamma_{\rm sh}^2$ (as measured in the upstream frame). This raises two questions: what is the ultimate source of magnetic amplification to that level? What sources the turbulence on the macroscopic scales $R/\Gamma_{\rm sh}^2 \sim 10^{13}(R/10^{17}\ {\rm cm})(\Gamma_{\rm sh}/100)^2$ cm? Current PIC simulations do indicate indeed that the above micro-instabilities can reach the required level of amplification, however there are other possibilities, such as the excitation of macroscopic turbulence through the interaction of the shock with upstream inhomogeneities [64], hydrodynamic instabilities of the blast itself [65,66] or even the self-reformation process of an oblique shock front. The latter question pertains to the lifetime of micro-turbulence that has been excited on skin depth scales $\sim 10^6$ cm, and whether it can survive up to macroscopic scales some eight orders of magnitude larger [67,51]. This question is yet unresolved. At this stage, one cannot exclude that the triggering of micro-instabilities opens the way for Fermi cycles, that produce the accelerated populations, yet, that these populations radiate synchrotron spectra on longer timescales in the emission region of size $R/\Gamma_{\rm sh}^2$, in a macroscopic magnetized turbulence that has been produced by another (macro-) instability.

6. High energy gamma rays, cosmic rays and neutrinos

Acceleration of particles to very high energies may produce very high energy cosmic rays and secondary products such as high energy gamma rays and neutrinos, that provide additional windows on the physics of acceleration. Let us briefly discuss these possibilities in turn.

6.1. High energy gamma rays

One of the most salient results of the Fermi-LAT telescope in the past few years has undoubtedly been the detection of high energy gamma rays with $E \sim 10$–100 GeV from long gamma-ray bursts, see for instance [68]. This detection has been translated into a stringent lower limit on the bulk Lorentz factor of the flow, $\Gamma_{\rm w} \gtrsim 1000$, arguing that otherwise the γ–γ optical depth would be too high to allow the escape of these high energy gamma rays. The origin of these gamma rays, whether synchrotron or inverse Compton and at what location, is also vividly debated. With respect to the acceleration process at play, it is very interesting to note that in order to produce a synchrotron spectrum extending to nearly 100 GeV, the acceleration timescale must not be larger than a Larmor time $t_{\rm L}$, meaning that it should operate in the Bohm regime [69]. However, this result is unexpected: if most of magnetic energy density is set on short spatial scales, the scattering timescale should increase in proportion to $t_{\rm L}^2/\ell_{\rm c}$, hence largely exceed the Bohm limit. These new observational results clearly open new avenues of research that will lead to significant developments in our understanding of gamma-ray burst physics and particle acceleration.

[2] Wakefield acceleration is a process whereby a particle, e.g. an electron is accelerated in the electrostatic field that is excited in the wake of a large amplitude electromagnetic wave propagating in an electron–ion plasma [60].

6.2. Neutrinos

There are three main channels of neutrino production in gamma-ray bursts (see [70] for a detailed discussion): (i) neutron β decay; (ii) inelastic nuclear collisions producing charged pions that decay to ν_μ, ν_e and their antiparticles; (iii) photohadronic interactions of low energy photons with high energy protons, that also lead to the production of charged pions, hence neutrinos. The latter channel is of greater interest to the present discussion as it would lead to the production of very high energy neutrinos, which offer an invaluable probe of acceleration physics. Of course, much would also be learned on gamma-ray burst phenomenology through the detection of $\sim$100 GeV neutrinos associated with channels (i) and (ii).

As protons are shock accelerated to large energies in the flow, they may interact with low energy photons produced during the prompt emission and produce pions. The threshold condition for pion production can be written $\sqrt{E_{\rm p}\epsilon_\gamma} \gtrsim 0.4\Gamma_{\rm w}$ GeV (both $E_{\rm p}$ and ϵ_γ are evaluated in the observer frame), see [71] for a detailed discussion. During the prompt phase, the flux peaks at observed energies $\epsilon_\gamma \sim 1$ MeV, so that neutrino production is optimal for protons of energies $E_{\rm p} \gtrsim 10^{16}$ eV, which produce neutrinos of energies $E_\nu \gtrsim 10^{14}$ eV (the outgoing neutrinos generally carry $\sim$5% of the parent proton energy). At lower proton (hence neutrino) energies, the threshold lies above the peak energy, hence there are less photons available for pion production, implying a fall-off of the optical depth as $E_{\rm p}$ decreases. If the accelerated proton spectrum has a differential slope s, then so does the neutrino spectrum above $\sim 10^{14}$ eV, with a slope typically $s-1$ below that energy.

The prospect for neutrino detection directly depends on the amount of energy contained in the accelerated ion population, which is unknown as, so far, only the leptonic contribution has been constrained by observations. If accelerated baryons carry as much energy as the observed photons, then the prospects for detection are rather dire, even with km^3 neutrino telescopes, with less than an event per year from the diffuse background. However, if one assumes that gamma-ray bursts are the sources of ultra-high energy cosmic rays above 10^{19} eV, as will be discussed in the following section, then the km^3 detectors may record 1–10 events per year. Such limits are now being probed by the Ice Cube experiment [72]. The corresponding neutrino flux is sometimes referred to as the Waxman–Bahcall bound [73], which assumes that the parent proton population flux is normalized to the ultrahigh energy cosmic ray flux, that it has a slope $s=2$ and that each source outputs as much energy in neutrinos as in protons, corresponding to the assumption of an optical depth to pion production of order unity. Certainly, a slightly larger spectral index, for instance $s \simeq 2.2$, would weaken significantly the expectations for the neutrino flux, because the energy contained in the high energy proton population above the threshold for photo-pion production would then be smaller at a given overall energy budget.

The prediction of a high energy neutrino flux during the afterglow is much more model dependent, notably because the modelling of the shock wave radiative efficiency and dynamics is subject to interpretation, following the discovery of the steep decay of the early X-ray afterglow, followed by a shallow phase with in some cases X-ray flares. Nevertheless, one can note that the typical observed photon energy is much smaller than during the prompt phase, hence the emitted energy flux $E_\nu^2 {\rm d}N_\nu/{\rm d}E_\nu$ is expected to peak at higher energies, as high as $E_\nu \sim 10^{18}$ eV (provided acceleration of protons can proceed to 10^{20} eV during that stage). Furthermore, since the target photon density falls off as the fireball expands, so does the fraction of energy lost to pion production, hence to neutrinos. All things being equal, one thus expects the neutrino afterglow flux to be weaker than that produced during the prompt phase. The recent study of [74] has made detailed calculations of the neutrino spectrum produced during that stage using various published theoretical models for the dynamics, which were designed to explain the features of the afterglow. The spectra obtained follow the tendency described above, with a rather strong model dependence of the flux and peak energy. Several experimental projects have been proposed or are currently trying to detect neutrinos at energies $\gtrsim 10^{18}$ eV, including the so-called GZK neutrinos that are associated with the pion production interactions of ultra-high energy cosmic rays on cosmic microwave background photons.

6.3. Very high energy cosmic rays

It has been remarked that if gamma-ray bursts output an equivalent amount of energy in gamma rays and in cosmic rays above 10^{19} eV, then these objects might account for the measured flux of ultrahigh energy cosmic rays between $\sim 3\times 10^{18}$ eV and $\sim 10^{20}$ eV [75–77]. This is all the more interesting as gamma-ray bursts seem to offer, on theoretical grounds, the prerequisite conditions for acceleration to the most extreme cosmic ray energies recorded (see below). With modern constraints on the local flux ($z=0$) of gamma-ray bursts, this coincidence has been somewhat revised toward more pessimistic estimates, in the sense that one would now require standard long high luminosity gamma-ray bursts to output at least ten times more energy in ultra-high energy cosmic rays than in photons. Even this figure is subject to debate, see for instance [78] and [79].

Concerning the mechanism of acceleration to ultra-high energies, one can list quite a few scenarios, among which: shock acceleration in mildly relativistic internal shocks or at the mildly relativistic reverse shock [77,71,80], Fermi acceleration at the ultra-relativistic external shock [76] (see however [21]), acceleration in relativistic turbulence, either in the internal shock phase [77] or behind the external forward shock [81], shear acceleration in the inner jet [4] or through repeated interactions with shock fronts in the internal shock phase [82,83]. Most of these models conclude to the possibility of pulling protons up to the 10^{20} eV limit, at the price of more or less optimistic hypotheses. Several pros and cons and some salient features are noteworthy.

If acceleration takes place at short radii, the opacity to pion production must be sufficient to allow the protons to escape the flow by turning into neutrons via photo-hadronic interactions, otherwise the protons would lose their energy through adiabatic expansion (unless the magnetization drops abruptly beyond the acceleration region, see [82] for a discussion). Therefore, the generation of a PeV neutrino signal is a generic prediction of models that accelerate ultra-high energy cosmic rays in the inner parts of gamma-ray bursts. As mentioned above, if each gamma-ray burst outputs as much energy into neutrinos than in protons, and these objects account for the bulk of the ultra-high energy cosmic ray flux, then the PeV neutrino signal lies within the reach of current detectors. Conversely, however, one could not rule out gamma-ray bursts as the sources of ultra-high energy cosmic rays, were this signal not detected.

At first look, acceleration at the external forward shock wave appears unlikely in the ultra-relativistic regime, for the following reasons. Taking the most optimistic acceleration timescale $t_{\rm acc} \simeq r_{\rm L}/(\Gamma_{\rm sh} c)$ with quantities measured in the upstream frame (see the discussion in [57]), an upper bound on the maximal energy can be derived by comparing $t_{\rm acc}$ with the dynamical timescale R/c, leading to $E_{\rm max} \lesssim 10^{20} \Gamma_{\rm sh,300} R_{16} \sigma_{\rm u}^{1/2}$ eV, where $\Gamma_{\rm sh,300} = \Gamma_{\rm sh}/300$, $R_{16} = R/10^{16}$ cm and $\sigma_{\rm u}$ denotes the upstream magnetization parameter, which takes the value 10^{-9} in the interstellar medium ($B \sim 3$ μG). Acceleration to ultra-high energies at the external forward shock thus requires an extremely high value of the magnetization. If such values pre-existed in the upstream medium, Fermi acceleration would not develop according to the discussion of Section 5. If this magnetization were generated through micro-instabilities, then one would expect $\sigma_{\rm u} \sim \epsilon_B \lesssim \epsilon_{\rm cr} < 1$, where as before ϵ_B denotes the fraction of downstream dissipated energy carried by the magnetic field, and $\epsilon_{\rm cr}$ the same ratio, albeit for the cosmic ray population; the last inequality follows from the fact that the magnetic field is seeded by the cosmic ray population itself. Furthermore, due to the microscopic nature of the electromagnetic turbulence, the acceleration timescale should increase quadratically with the particle energy and thus become quite large at high energies. This would prohibit acceleration to the energies required. Thus at this stage of the description of collisionless relativistic shocks, one would not expect acceleration of ultra-high energies at the external ultra-relativistic shocks. Nevertheless, it is interesting to note that the steep decay of the early X-ray afterglow has been interpreted as some form of haemorrhage of the blast energy through the production and escape of cosmic rays [84].

Alternatively, acceleration might take place at the reverse external shock wave, which is mildly relativistic and thus does not suffer from the limitations of ultra-relativistic Fermi acceleration discussed above.

On more general grounds, one may derive a useful bound on the magnetic luminosity L_B of a source of ultra-high energy cosmic rays [85–87]. Assuming that acceleration takes place in an outflow and writing the acceleration timescale as a multiple of the Larmor time, one can show that $L_B \gtrsim 10^{45}$ erg/s is a necessary condition in order to reach 10^{20} eV. The exact inequality for L_B actually contains numerical prefactors that are larger than unity, so the exact bound is actually more stringent (up to a dependence Z^{-2} on the charge of the accelerated particle). This offers a strong constraint on possible sources of ultra-high energy protons, which severely limits the class of candidates. In terms of phenomenology, if ultra-high energy cosmic rays are protons – existing claims on the chemical composition are at present contradictory – then transient sources such as gamma-ray bursts or possibly newly born magnetars are favored candidates for the origin of these extreme cosmic rays, as no correlation has been observed with radio-loud quasars or FR-II radio-galaxies, see the discussion in [87].

7. Discussion, open questions and perspectives

Thanks to the conversion of a fraction of the ultra-relativistic kinetic energy of the outflow into accelerated particles, gamma-ray bursts are sources of very high energy phenomena, high energy gamma rays, most likely high energy cosmic rays and potentially high energy neutrinos. It is generally expected that the extension of the Fermi acceleration mechanism – seemingly so successful in supernovae remnant non-relativistic shocks – to the relativistic domain would account for this conversion, at least at the external forward shock wave. Indeed, detailed observations have revealed power law distributions of highly energetic electrons and brought forward evidence for intense amplification or generation of magnetic fluctuations. So, Nature has solved this acceleration problem. From the point of view of theory, however, pessimism has been raised on the very efficiency of relativistic Fermi acceleration… How exactly does this process occur thus remains the subject of active studies, both analytical and numerical. In particular, very substantial progress has been achieved in our understanding of the generation of magnetic fluctuations at relativistic collisionless shocks, which are of paramount importance to the success of Fermi acceleration. Such instabilities must develop on short scales, likely in the kinetic regime or short scale MHD, as otherwise they would not provide sufficient scattering to allow Fermi power laws to emerge. Fortunately, current Particle-In-Cell simulations now allow to construct ab initio collisionless shocks with near realistic physical conditions and they have even shed some light on the generation of Fermi power laws of accelerated particles. These are thus exquisite tools to perform detailed numerical experiments.

Many questions remain open, as we have stressed throughout this section. From smaller to larger scales: what are the most relevant instabilities and what are their relation to the collisionless shock structure? How do accelerated particles interact with this turbulence, i.e. what are the scattering and acceleration rates that are tightly constrained by the observations of high energy synchrotron radiation (X-ray, possibly up to the gamma domain)? A somewhat related question, what is the maximal energy that can be achieved in ultra-relativistic shock acceleration? Can it produce ultra-high energy cosmic rays? What is the expected spectral index of relativistic Fermi acceleration? What is the structure of the turbulence downstream of the shock? In particular, do the instabilities account for the level of amplification inferred from the synchrotron modelling of gamma-ray bursts afterglows? Does the turbulence, that is excited on microscopic skin depth scales, survive on

sufficiently long timescales in order to explain the apparent emission on macroscopic spatial scales? Or, is the macroscopic turbulence produced through some other large scale instability?

As we have tried to emphasize throughout this article, the detailed analysis of gamma-ray bursts observations in various wavebands, as well as multi-messenger studies of gamma-ray bursts with cosmic ray and neutrino detectors may well ultimately provide answers to many of the above questions. Thanks to the upcoming generations of instruments, the future does indeed look bright in that respect.

Acknowledgement

We acknowledge financial support by the PEPS-PTI program of the CNRS Physics Institute (INP).

References

[1] T. Piran, Rev. Mod. Phys. 76 (2005) 1143.
[2] M. Lyutikov, R. Blandford, eprint, arXiv:astro-ph/0312347, 2003.
[3] R. Narayan, P. Kumar, Month. Not. Roy. Astron. Soc. 394 (2009) 117.
[4] F.M. Rieger, P. Duffy, Astrophys. J. 632 (2005) L21.
[5] E. Fermi, Phys. Rev. 75 (1949) 1169.
[6] G. Pelletier, Astron. Astrophys. 350 (1999) 705.
[7] V.S. Berezinskii, S.V. Bulanov, V.A. Dogiel, V.S. Ptuskin, Astrophysics of Cosmic Rays, North-Holland, 1990.
[8] F. Aharonian, et al., HESS Collaboration, Nature 432 (2004) 75.
[9] F. Aharonian, et al., HESS Collaboration, Astron. Astrophys. 516 (2010) 62.
[10] E.G. Berezhko, L.T. Ksenofontov, H.J. Völk, Astron. Astrophys. 505 (2009) 169.
[11] A.R. Bell, Month. Not. Roy. Astron. Soc. 182 (1978) 147.
[12] R. Blandford, D. Eichler, Phys. Rep. 154 (1987) 1.
[13] P.-O. Lagage, C. Césarsky, Astron. Astrophys. 125 (1983) 249.
[14] D.C. Ellison, D. Eichler, Phys. Rev. Lett. 55 (1985) 2735.
[15] E.G. Berezhko, L.T. Ksenofontov, H.J. Völk, Astron. Astrophys. 412 (2003) L11.
[16] I. Lerche, Astrophys. J. 147 (1967) 689.
[17] A. Bell, Month. Not. Roy. Astron. Soc. 353 (2004) 550.
[18] G. Pelletier, M. Lemoine, A. Marcowith, Astron. Astrophys. 453 (2006) 181.
[19] V.N. Zirakashvili, V.S. Ptuskin, H.J. Völk, Astrophys. J. 678 (2008) 255.
[20] V.N. Zirakashvili, V.S. Ptuskin, Astrophys. J. 678 (2008) 939.
[21] Y. Gallant, A. Achterberg, Month. Not. Roy. Astron. Soc. 305 (1999) L6.
[22] A. Achterberg, Y. Gallant, J.G. Kirk, A.W. Guthmann, Month. Not. Roy. Astron. Soc. 328 (2001) 393.
[23] L. Sironi, A. Spitkovski, eprint, arXiv:1009.0024, 2010.
[24] K.R. Ballard, A.F. Heavens, Month. Not. Roy. Astron. Soc. 259 (1992) 89.
[25] J. Bednarz, M. Ostrowski, Phys. Rev. Lett. 80 (1998) 3911.
[26] M. Lemoine, G. Pelletier, Astrophys. J. 589 (2003) L73.
[27] D.C. Ellison, G.P. Double, Astropart. Phys. 22 (2004) 323.
[28] J. Niemiec, M. Ostrowski, Astrophys. J. 610 (2004) 851.
[29] M. Lemoine, B. Revenu, Month. Not. Roy. Astron. Soc. 366 (2006) 635.
[30] J. Kirk, A. Guthmann, Y. Gallant, A. Achterberg, Astrophys. J. 542 (2000) 235.
[31] U. Keshet, E. Waxman, Phys. Rev. Lett. 94 (2005) 111102.
[32] J. Niemiec, M. Ostrowski, Astrophys. J. 641 (2006) 984.
[33] J. Niemiec, M. Ostrowski, M. Pohl, Astrophys. J. 650 (2006) 1020.
[34] M. Lemoine, G. Pelletier, B. Revenu, Astrophys. J. 645 (2006) L129.
[35] M.C. Begelman, J.G. Kirk, Astrophys. J. 353 (1990) 66.
[36] E. Waxman, Astrophys. J. 485 (1997) L5.
[37] R.A.M.J. Wijers, T.J. Galama, Astrophys. J. 523 (1999) 177.
[38] Z. Li, E. Waxman, Astrophys. J. 651 (2006) L328.
[39] Z. Li, eprint, arXiv:1004.0791, 2010.
[40] G. Pelletier, M. Lemoine, A. Marcowith, Month. Not. Roy. Astron. Soc. 393 (2009) 587.
[41] M. Milosavljević, E. Nakar, Astrophys. J. 651 (2006) 979.
[42] A. Spitkovsky, AIP Conf. Proc. 801 (2005) 345.
[43] A. Spitkovsky, Astrophys. J. 682 (2008) L5.
[44] T.N. Kato, Astrophys. J. 668 (2007) 974.
[45] P. Chang, A. Spitkovsky, J. Arons, Astrophys. J. 674 (2008) 378.
[46] M.E. Dieckmann, P.K. Shukla, L.O.C. Drury, Astrophys. J. 675 (2008) 586.
[47] K.-I. Nishikawa, J. Niemiec, P.E. Hardee, M. Medvedev, H. Sol, Y. Mizuno, B. Zhang, M. Pohl, M. Oka, D.H. Hartmann, Astrophys. J. 698 (2009) L10.
[48] U. Keshet, B. Katz, A. Spitkovsky, E. Waxman, Astrophys. J. 693 (2009) L127.
[49] T. Haugboelle, eprint, arXiv:1007.5082, 2010.
[50] L. Sironi, A. Spitkovski, Astrophys. J. 698 (2009) 1523.
[51] M.V. Medvedev, A. Loeb, Astrophys. J. 526 (1999) 697.
[52] J. Wiersma, A. Achterberg, Astron. Astrophys. 428 (2004) 365.
[53] Y. Lyubarsky, D. Eichler, Astrophys. J. 647 (2006) L1250.
[54] A. Achterberg, J. Wiersma, Astron. Astrophys. 475 (2007) 1.
[55] A. Bret, Astrophys. J. 699 (2009) 990.
[56] A. Bret, M.-C. Firpo, C. Deutsch, Phys. Rev. Lett. 94 (2005) 115002.
[57] M. Lemoine, G. Pelletier, Month. Not. Roy. Astron. Soc. 402 (2010) 321.
[58] B. Reville, J.G. Kirk, P. Duffy, Plasma Phys. Contr. Fus. 48 (2006) 1741.
[59] M. Hoshino, J. Arons, Phys. Fluids B 3 (1991) 818.

[60] T. Tajima, J.M. Dawson, Phys. Rev. Lett. 43 (1979) 267.
[61] Y. Lyubarsky, Astrophys. J. 652 (2006) 1297.
[62] M. Hoshino, Astrophys. J. 672 (2008) 940.
[63] M.V. Medvedev, Astrophys. J. 540 (2000) 704.
[64] L. Sironi, J. Goodman, Astrophys. J. 671 (2007) 1858.
[65] A. Levinson, Astrophys. J. 705 (2009) L213.
[66] W. Zhang, A. MacFadyen, P. Wang, Astrophys. J. 692 (2009) L40.
[67] A. Gruzinov, E. Waxman, Astrophys. J. 511 (1999) 852.
[68] A. Abdo, et al., Fermi Collaboration, Science 323 (2009) 1688.
[69] X.-Y. Wang, Z. Li, Z.-G. Dai, P. Mészáros, Astrophys. J. 698 (2009) L98.
[70] E. Waxman, Phil. Trans. Roy. Soc. A 365 (2007) 1323.
[71] E. Waxman, Lect. Notes Phys. 576 (2001) 122.
[72] R. Abbasi, et al., Ice Cube Collaboration, Astrophys. J. 710 (2010) 346.
[73] E. Waxman, J. Bahcall, Phys. Rev. D 59 (1999) 023002.
[74] K. Murase, Phys. Rev. D 76 (2007) 123001.
[75] M. Milgrom, V. Usov, Astrophys. J. 449 (1995) L37.
[76] M. Vietri, Astrophys. J. 478 (1995) L9.
[77] E. Waxman, Phys. Rev. Lett. 75 (1995) 386.
[78] B. Katz, R. Budnik, E. Waxman, J. Cosmol. Astropart. Phys. 03 (2009) 020.
[79] D. Eichler, D. Guetta, M. Pohl, eprint, arXiv:1007.3742, 2010.
[80] C.D. Dermer, S. Razzaque, eprint, arXiv:1004.4249, 2010.
[81] C.D. Dermer, M. Humi, Astrophys. J. 556 (2001) 479.
[82] D. Gialis, G. Pelletier, Astron. Astrophys. 425 (2004) 395.
[83] D. Gialis, G. Pelletier, Astron. Astrophys. 627 (2005) 868.
[84] C.D. Dermer, Astrophys. J. 664 (2007) 384.
[85] E. Waxman, Phys. Script. T 121 (2005) 147.
[86] M. Lyutikov, R. Ouyed, Astropart. Phys. 27 (2007) 473.
[87] M. Lemoine, E. Waxman, J. Cosmol. Astropart. Phys. 11 (2009) 009.